

Computational Investigation in Two-Phase Flow Dynamics of Highly Subcooled Flow Boiling Using FC-72 Dielectric Fluid in Vertical Up-flow

Submitted By

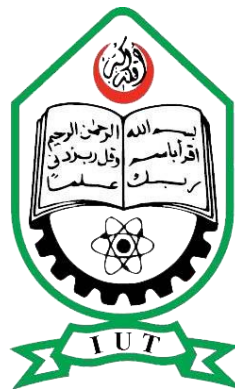
Mohammad Ishraq Hossain

180011132

Supervised By

Dr. Arafat Ahmed Bhuiyan

A Thesis submitted in partial fulfillment of the requirement for the degree of Bachelor of Science in Mechanical Engineering



Department of Mechanical and Production Engineering (MPE)

Islamic University of Technology (IUT)

May, 2023

Candidate's Declaration

This is to certify that the work presented in this thesis, titled, "Computational Investigation in Two-Phase Flow Dynamics of Highly Subcooled Flow Boiling Using FC-72 Dielectric Fluid in Vertical Up-flow", is the outcome of the investigation and research carried out by me under the supervision of Dr. Arafat Ahmed Bhuiyan, Associate Professor, MPE Dept., IUT
Furthermore, it is stated that neither this thesis nor any portion of it has been presented elsewhere to obtain any degree or diploma



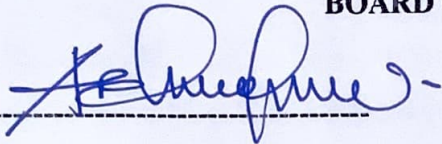
Mohammad Ishraq Hossain


Student No: 180011132

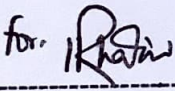
RECOMMENDATION OF THE BOARD OF SUPERVISORS

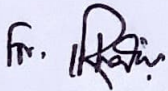
The thesis titled "Computational Investigation in Two-Phase Flow Dynamics of Highly Subcooled Flow Boiling Using FC-72 Dielectric Fluid in Vertical Up-flow" submitted by Mohammad Ishraq Hossain, Student No: 180011132 has been accepted as satisfactory in partial fulfillment of the requirements for the degree of B Sc. in Mechanical Engineering.

BOARD OF EXAMINERS

1. 

Dr. Arafat Ahmed Bhuiyan (Supervisor)
Associate Professor
MPE Dept., IUT, Board Bazar, Gazipur-1704, Bangladesh.
2. 

Dr. Md. Rezwanul Karim (Examiner)
Associate Professor
MPE Dept., IUT, Board Bazar, Gazipur-1704, Bangladesh.
3. 

Dr. Mohammad Monjurul Ehsan (Examiner)
Associate Professor
MPE Dept., IUT, Board Bazar, Gazipur-1704, Bangladesh.
4. 

Fahim Tanfeez (Examiner)
Lecturer
MPE Dept., IUT, Board Bazar, Gazipur-1704, Bangladesh.

Acknowledgment

I would like to extend my warmest gratitude to my undergraduate thesis supervisor Dr. Arafat Ahmed Bhuiyan, for his kindest supervision during my final year. He proved to be an invaluable resource in this journey starting from formulating the research topic to finally doing all the necessary work for completion. His uncompromising principle of perseverance guided me through all the hurdles along the way. I would also like to thank my senior and peers of MPE Department of IUT for all their technical help in creating my CFD model. Their support and encouragement helped me cross the finish line. I am quite proud of this year long struggle by me accomplished through organic learning. Hopefully this experience will prove quite helpful in my future endeavors in graduate level research.



Mohammad Ishraq Hossain

Abstract

This computational simulation examines the flow of a specific dielectric electronic cooling fluid, FC-72, as it boils in a narrow channel with two opposing walls that supply heat at different rates. The heat flux provided by the walls is between 42-45% of the critical heat flux. The physical experiment with which the numerical data is compared with involved measuring local wall temperatures at various points along the channel and using this information to determine the heat transfer coefficient. The flow patterns and phases present are also observed. The results of a previously done experiment is compared with the predictions made by computer simulation using ANSYS FLUENT. The numerical calculations have been based on multiphase VOF model along with Lee model as the phase transition mechanism. The simulation takes into account the movement of the liquid and gas phases and heat transfer along the walls and the effect of gravity on fluid.

Contents

1. Introduction.....	10
1.1 Background.....	10
1.2 Advent of two-phase thermal cooling systems.....	11
1.3 Effectiveness of Flow boiling configuration	12
1.4 Modelling techniques	12
1.5 Computation approaches to anticipate heat flux phenomena	14
1.6 Objectives of this Study	14
2. Numerical Methodology.....	15
2.1 Mathematical depiction and computational specifics	15
2.2 Computational Domain	16
2.3 Grid independence test.....	18
2.4 Initial Boundary Conditions	19
2.5 Phase Change Model.....	19
3. Results and Discussions	21
3.1 Flow Characteristics in sub-cooled boiling.....	21
3.1.1 Results of Flow Visualization	21
3.1.2 Distribution of void fraction and velocity profiles in the transverse and longitudinal directions of the channel.....	24
3.2 Heat transfer characteristics in sub-cooled boiling.....	25
4. Future Work.....	30
5. Conclusions.....	30
References	31

List of Figures

Figure 1: Schematic of Computational Domain	17
Figure 2: Validation of Grid Independence via Temporal Average of Wall Temperature	18
Figure 3: Experimental [30] flow images of channel at 10ms time apart in test case 2 [$G = 836.64 \text{ kg/m}^2\text{s}$].....	23
Figure 4: Analyzing for test Case 2 by Evaluating the Consistency between Empirical and Computational Axial Profiles of Average Void Fraction.....	24
Figure 5: Comparison of time-averaged transverse void fraction profile along different axial locations.....	25
Figure 6: Comparison of experimental and computational axis variations of wall temperature for test case 2	26

List of Tables

Table 1: Input conditions of the three test cases	19
Table 2: Corresponding thermophysical properties of FC-72 used in the three test cases	20
Table 3: Numerical details and discretization methods.	21

Nomenclature and Symbols

c_p	specific heat at constant pressure
Δc	mesh (cell) size
E	energy per unit mass
e	parameter in Smith model
F	force per unit volume
G	mass velocity
g	gravitational acceleration
H	larger width of flow channel's cross-section
h	heat transfer coefficient
h_{fg}	latent heat of vaporization
I	turbulent intensity
k	thermal conductivity
k_{eff}	effective thermal conductivity
L_d	upstream development length of flow channel
L_e	exit length of flow channel
$L_{e,c}$	added exit length in computational domain
L_h	heated length of flow channel
\dot{m}	volumetric mass source

Greek Symbols

α	volume fraction; void fraction
μ	dynamic viscosity
ν	kinematic viscosity
ρ	density
σ	surface tension
φ	property

Subscripts

f	liquid
g	vapor
i	index for phase
in	inlet to heated portion of flow channel
sat	saturation
$wall$	wall

1. Introduction

1.1 Background

The study of compact cooling technologies capable of handling high heat fluxes has gained momentum due to the increasing heat generation rates in various high-power devices. The primary focus of NASA's present Strategic Plan revolves around sending astronauts on Lunar missions [Lunar gravity ($0.17 g_e$)] and Mars [Martian gravity ($0.38 g_e$)], necessitating next-generation spacecraft that are both high-powered and lightweight [1]. As a result of this necessity, there is an increased production of heat at the component, module, and system scales. Effective dissipation of excessive heat is crucial for aerospace devices as their working temperature significantly impacts accuracy, reliability, and lifespan. One promising approach for these applications is the utilization of Mini-channel or Micro-channel heat transfer systems [2]. In phase-change scenarios, these arrangements of such systems provide space efficiency, a substantial ratio of surface area to volume, an elevated aspect ratio, and minimal coolant consumption. Compared to single-phase systems, flow boiling in Mini-channels/Micro-channels exhibits a higher heat transfer coefficient and allows for a nearly constant surface temperature determined by the fluid's saturation temperature [3]. Traditionally, most research on two-phase heat transfer has focused on water boiling under atmospheric or under elevated pressures in power plant settings [4]. However, the use of water as a cooling agent is restricted due to its quite elevated boiling point, which makes it unsuitable for electronic devices that require lower peak temperatures. To overcome this limitation, one option is to operate the boiling system with water at reduced pressures, while another approach is to use alternative coolants with lower boiling temperatures [5]. FC-72 is an appealing coolant for achieving low operating temperatures [6]. FC-72 possesses excellent thermal and chemical stability, along with being nonflammable and highly safe due to its negligible toxicity, rendering it highly suitable for low-temperature applications. Its boiling point is 56°C at atmospheric pressure (which further decreases under sub-atmospheric conditions). Despite having a lower latent heat of 93 kJ/kg (at 56°C saturation temperature) compared to water, FC-72 exhibits comparable cooling performance to numerous alternative refrigerants. [7].

1.2 Advent of two-phase thermal cooling systems

The growing demand for higher heat fluxes and the heightened influence of operating temperature in advanced high-power systems highlight the inadequacy of conventional single-phase cooling techniques to fulfill cooling needs. Consequently, there has been a notable shift towards exploring two-phase thermal management strategies, wherein heat is acquired through boiling and dissipated through condensation. These two-phase approaches offer enhanced heat transfer coefficients by effectively utilizing both the sensible and latent heat of the cooling medium. [8]. In the majority of such systems, heat dissipation from high-flux surfaces relies on boiling, with the resulting liquid-vapor mixture directed to a condenser for ambient heat rejection, thus restoring the vapor to its liquid form. Given the growing attention towards two-phase systems, it is imperative to expedite the development of precise predictive design software [9]. Important considerations in the development of thermal management systems involving two-phase flow include the coefficient of heat transfer, pressure drop and the CHF. Surpassing the CHF threshold can result in catastrophic malfunction of the heat-dissipating apparatus, instigating an abrupt and unstable rise in device temperature, thereby risking overheating or complete physical failure [10].

A critical research requirement for upcoming space missions involves the reduction of the overall weight of subsystems in space vehicles. One key subsystem is the Thermal Control System (TCS), responsible for regulating temperature and humidity within vehicles and planetary bases [11]. The TCS fulfills three primary roles: heat collection, heat transfer, and heat dissipation. Components responsible for heat collection gather heat from diverse origins and convey it into the TCS loop, while heat transfer components facilitate the movement of heat towards the heat dissipation components. Subsequently, the heat dissipation components emit the heat into the vast expanse of space. In contrast to existing TCS technologies that depend solely on the sensible heat increase of the working fluid for heat removal, a two-phase TCS capitalizes on both sensible and latent heat, resulting in markedly enhanced heat transfer efficiency and reduced system weight in comparison to single-phase TCS systems. [12]. Understanding the impact of reduced gravity on two-phase fluid physics and heat transfer is therefore essential for developing an efficient two-phase TCS [13]. The importance of dual-phase fluid dynamics and thermal exchange in forthcoming space expeditions is apparent based on the conclusions of a multitude of studies. These investigations have specifically recommended the application of flow boiling and condensation in space propulsion, thermal

control, and state of the art life support systems

1.3 Effectiveness of Flow boiling configuration

In the context of reduced gravity, the presence of vapor on the heat-dissipating surface poses significant challenges for pool boiling [14]. Similarly, falling film cooling, which relies on gravity, is not a feasible option for heat acquisition in such conditions. Moreover, conventional boiling configurations that utilize mechanical pumps to circulate coolant and prevent vapor accumulation encounter various difficulties when implemented in reduced gravity. For instance, employing microchannels, jets, or sprays can lead to significant pressure drops across the boiling module [15]. Additionally, ensuring surface temperature uniformity often necessitates the use of multiple jet arrays, resulting in increased coolant flow rate and pumping power. Implementing sprays is challenging due to the inability to remove spent liquid after impact in the absence of gravity. Consequently, channel flow boiling emerges as the most effective method for thermal management in reduced gravity, offering advantages such as minimal pressure loss, a moderate rate of coolant flow, and convenient integration inside a boiling module [16]. In two-phase space systems, flow boiling offers a viable solution to counterbalance the absence of gravitational force, as it utilizes the movement of the liquid in bulk to displace bubbles from the surface, thereby preventing the formation of a large vapor void [17].

1.4 Modelling techniques

The current investigation pertains to the characteristics of two-phase flow and heat transfer in a channel supplied with a subcooled liquid coolant (below saturation temperature). Utilizing both sensible and latent heat, subcooled boiling presents benefits in terms of enhanced heat transfer performance. Furthermore, it effectively sustains a reduced void fraction within the flow channel, particularly under high mass velocities, thus mitigating the amplification of pressure drop and postponing the occurrence of critical heat flux (CHF). However, understanding the heat transfer mechanisms in subcooled flow boiling is not as comprehensive as in saturated flow boiling because of the pronounced lack of equilibrium between the liquid and vapor phases, it results in a substantial non-equilibrium condition.

Significant research endeavors have been directed towards the measurement and prediction of transitional parameters in subcooled flow boiling, such as the onset of nucleate boiling (ONB) [18] onset of significant void (OSV) [19] and onset of flow instability (OFI) [20]. Investigating changes in wall temperature and heat transfer coefficient throughout the channel is of significant importance. Gaining insights into these spatial variances necessitates establishing a connection between heat transfer properties and the evolution of the delicate near-wall vapor void layer along the heated surface, which proves to be a difficult task to accomplish experimentally in subcooled flow conditions. The gradual axial enlargement of this boundary due to bubble formation and coalescence can result in a persistent vapor layer along the downstream portions of the channel wall, serving as a precursor to the occurrence of Critical Heat Flux. [21].

Typically, subcooled flow boiling initiates with a liquid phase prevailing at the entrance of the channel. As the liquid progressively heats up adjacent to the channel wall, bubble formation occurs during the initiation of nucleate boiling as the wall temperature exceeds the saturation temperature. Given that the majority of the liquid is considerably cooler than the saturation temperature, the bubbles undergo substantial condensation, restricting their reach into the main region. As the liquid in the main region becomes progressively warmer downstream, condensation diminishes, and the expansion of the bubble layer results in observable penetration into the main flow, known as observable surface voiding. The transition from subcooled to saturated boiling may occur as the bubble layer undergoes downstream coalescence and growth, depending on various factors such as mass velocity, quality, channel geometry, heat transfer & inlet pressure.

Scientists have employed diverse approaches to anticipate the heat transfer characteristics in subcooled flow boiling [22]. These approaches incorporate experimental relationships involving limited applicability, analytical models (including semi-empirical), and computational models. Recently, the use of "universal correlations" has gained popularity in designing two-phase thermal management systems [23]. These correlations rely on extensive databases encompassing a broad spectrum of fluids, inlet conditions, mass velocities, channel dimensions, lengths, and wall heat fluxes obtained from multiple sources.

1.5 Computation approaches to anticipate heat flux phenomena

Computational methods have had a lot of success in the past decades accurately predicting the flow characteristics and heat flux of single-phase fluids, demonstrating successful correlation with experimental results across a wide range of flow configurations. These methods have improved over time and became more user-friendly and robust. However, these methods have not been as successful in predicting two-phase flow, especially when there is a phase change involved. While empirical correlations and experimental studies have been extensively employed for single-phase applications, the utilization of such methods is limited when it comes to two-phase applications. A study by Kharangate et al [24], progress in computational techniques to model flows involving two phases has been restricted to basic setups, like pool boiling and the impact of individual droplets on thermally enhanced surfaces, thus yielding limited achievements. Moreover, the majority of computational tools used for analyzing dual phase flow require extensive computation time and necessitate high-performance computational resources, even for relatively simple models. Considering the intricate nature of phase transition phenomena, there is a pressing need to enhance the capabilities of these tools in order to address significant factors such as bubble departure, coalescence and growth, turbulence, interfacial waviness and the accurate prediction of the onset of nucleate boiling and critical heat flux, particularly for complex flow geometries. In order to accomplish this, several crucial research objectives must be pursued by investigators before an accurate methodology can be developed. The primary hurdles in enhancing the accuracy of two-phase computational models lie in the precise tracking of interfaces and the modeling of phase change. Two commonly employed models for modeling two-phase flows are the Eulerian and Lagrangian methods [25]. Of the two Eulerian model is best suited for the computational model of this particular case.

1.6 Objectives of this Study

The aim of this numerical investigation is to gather data on flow boiling in earth gravity of 9.81 m/s^2 , subsequently used to develop predictive tools for pressure drop and heat transfer in straight channels. The focus of this study is on flow boiling, and the goal is to establish a foundation for predicting flow boiling with subcooled inlet conditions. Previous experiments

in Earth gravity have shown that bubble coalescence leads to the development of an undulating vapor film along the heated surface, which is a precursor to CHF, a critical design considerations and safety parameters for heat flux-controlled surfaces in both terrestrial and space applications. In this research, a computational analysis will be conducted to examine the behavior of fluid flow and heat transfer during subcooled boiling of FC-72 in a rectangular channel with upward vertical flow. The focus will be on studying the formation of the undulating vapor layer under various conditions of mass flux and wall heat fluxes. To verify the accuracy of the phase change model employed in the computational analysis, vapor void fraction measurements will be employed. The selection of a vertical upward flow orientation is grounded on its capacity to uphold flow symmetry within a channel subjected to heating from opposing directions. To anticipate the temperature of the channel wall and the heat transfer coefficient, a combination of temporal and spatial averaging methods will be employed.

2. Numerical Methodology

2.1 Mathematical depiction and computational specifics

We utilize the transient VOF method [26] in ANSYS FLUENT [27] in order to observe the dynamics of the interface in flow boiling and consider the exchange of mass between the two phases, the volume of fluid model is employed. This model determines the volume occupied by each phase within a cell, with the volume fraction representing the proportion of each phase present. The sum of the volume fractions of the two phases always equals one. Density variations are disregarded due to the assumption of incompressible flow. Through the resolution of the volume fraction's continuity equation, the interface is continuously tracked across the computational domain.

For liquid phase,

$$\frac{\partial \alpha_f}{\partial t} + \nabla \cdot (\alpha_f \vec{u}_f) = \frac{1}{\rho_f} \sum (\dot{m}_{gf} - \dot{m}_{fg})$$

and vapor phase,

$$\frac{\partial \alpha_g}{\partial t} + \nabla \cdot (\alpha_g \vec{u}_g) = \frac{1}{\rho_g} \sum (\dot{m}_{fg} - \dot{m}_{gf})$$

The combined phase momentum and energy equations are given by,

$$\frac{\partial}{\partial t} (\rho \vec{u}) + \nabla \cdot (\rho \vec{u} \vec{u}) = -\nabla P + \nabla \cdot [\mu (\nabla \vec{u} + \nabla \vec{u}^T)] + \vec{F},$$

and

$$\frac{\partial}{\partial t} (\rho E) + \nabla \cdot (\vec{u} (\rho E + P)) = \nabla \cdot (k_{eff} \nabla T) + S_h,$$

where E (J/kg) is energy per mass.

The subcooled flow boiling in channels is addressed by utilizing an implicit formulation that incorporates body forces to consider the separation of vapor and recovery of liquid in the wall region. The modeling of surface tension and wall adhesion is accomplished through the application of the Continuum Surface Force method [28]. To incorporate the impacts of turbulent phenomena, the two-equation Shear Stress Transport (SST) k - ω turbulence model is used [29], with a turbulence damping factor of 10, and the Low Reynolds-Number correction for turbulent viscosity damping is also applied.

2.2 Computational Domain

We examine a two-dimensional flow channel with specific dimensions, as illustrated in Figure 1. The channel has a fluid region of 5 mm by 144.6 mm and two solid walls that measure 1.04 mm by 114.6 mm. The computational model's dimensions correspond to the experimental flow boiling setup of the study by Lee et al [30], with the exception of the fluid domain length extended by an additional 30 mm to eliminate any influences from the outlet. This extra fluid length is inert in terms of thermal activity and does not involve solid meshes. Within the computational domain, there are two solid meshes, each measuring 1.04 mm in thickness, serving as representations of the copper heating walls. These meshes facilitate the examination of exchange of thermal energy between the solid medium and the fluid region. The entire

domain is divided into a non-uniform quadrilateral mesh, which is refined towards the walls to accurately capture miniature vapor voids. The 2D rectangular channel mesh is generated using ANSYS MESH.

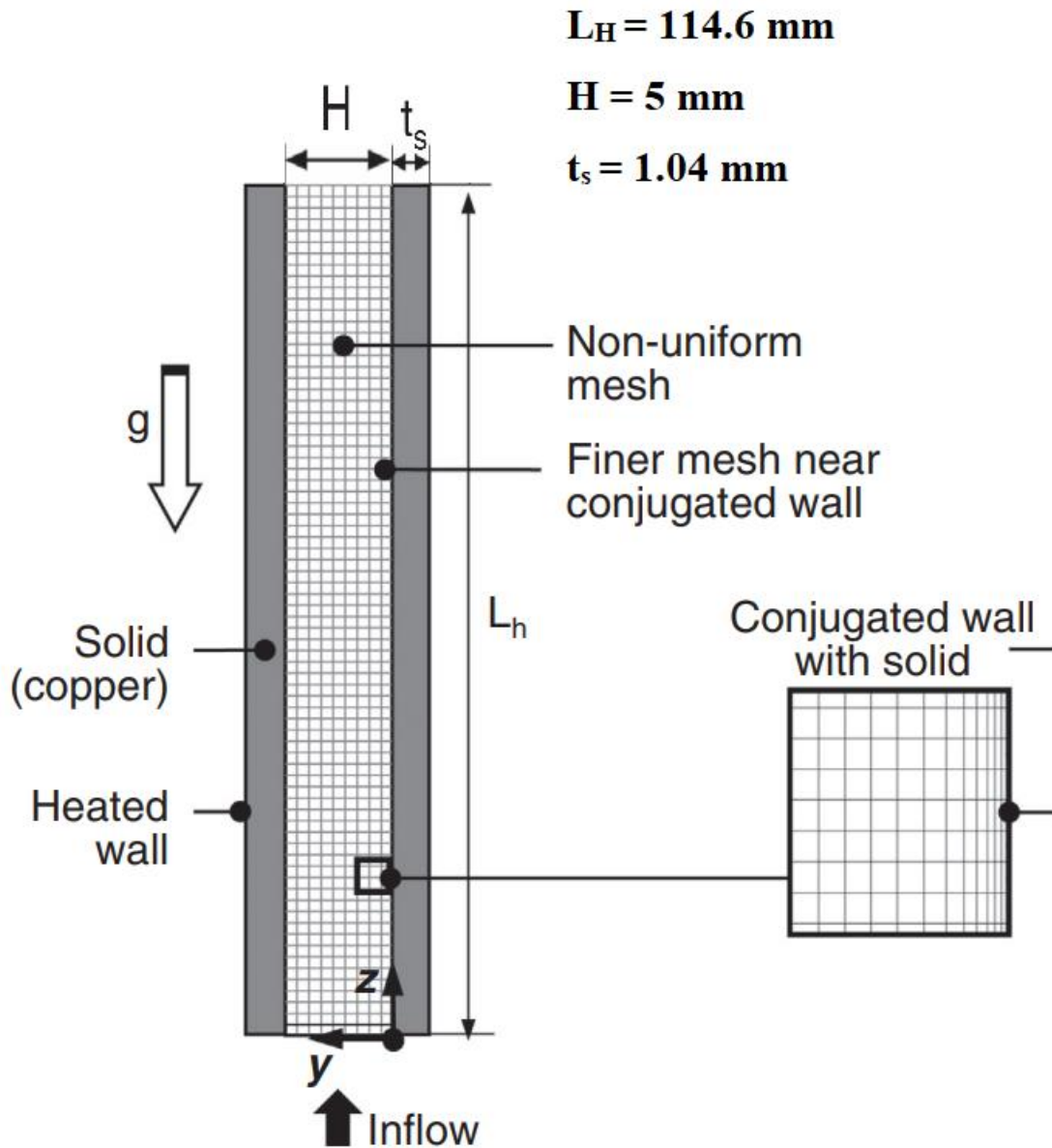


Figure 1: Schematic of Computational Domain

2.3 Grid independence test

To ensure grid independence, a test scenario is carried out with a mass velocity of $G = 836.64 \text{ kg/m}^2\text{s}$. Various mesh configurations with various cell sizes near the channel wall are modeled, and the mean temperature of the channel wall across space is calculated at specific measurement points ($z = 5.4, 22.7, 40, 57.3, 74.6, 91.9, \text{ and } 109.2 \text{ mm}$) once a steady state is attained. The obtained temperature values are subsequently compared with the corresponding empirical data. As depicted in Figure 3, it can be observed that the averaged wall temperature achieves asymptotic convergence when the near-wall cell size is smaller than approximately 10^{-4} m . In this study, a cell size of $\Delta c = 1 \times 10^{-4} \text{ m}$ is used in the bulk flow region and the same used in the near wall region to avoid the heavy computational load that comes with such mesh interfaces.

Data for experimental model is taken from the study conducted Lee et al [30]

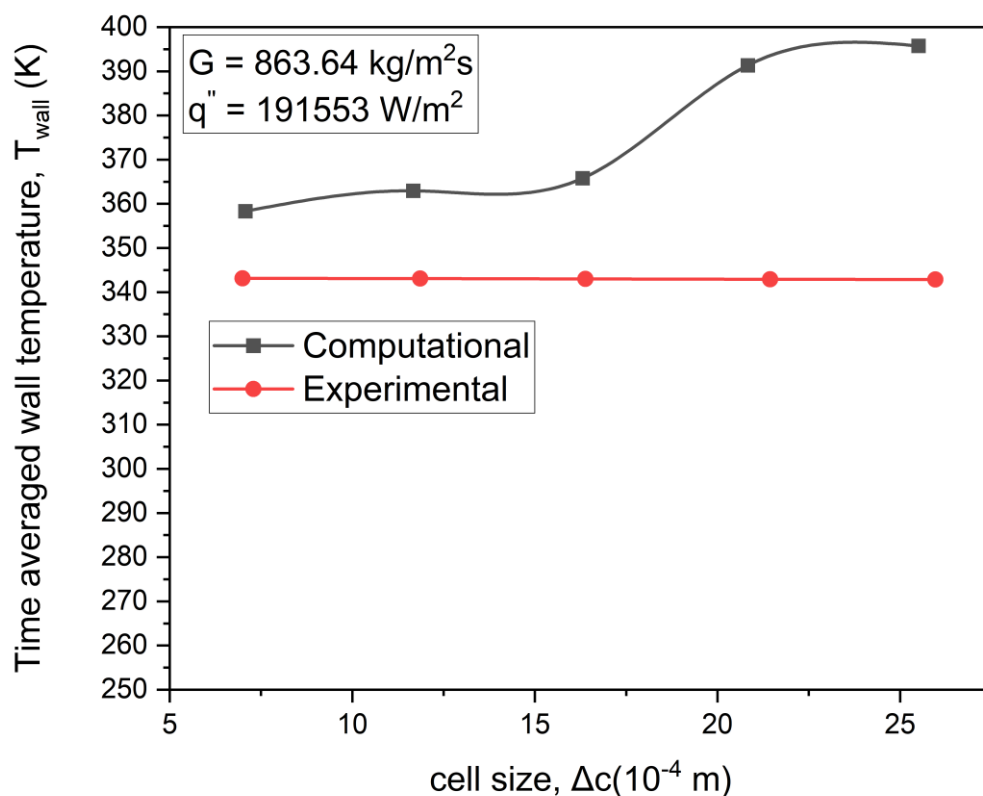


Figure 2: Validation of Grid Independence via Temporal Average of Wall Temperature

2.4 Initial Boundary Conditions

In this experiment, the focus is on studying the impact of varying mass velocities and wall heat flux on flow boiling and condensation. The computational model used in the analysis does not include the initial section of the channel where the fluid is not yet fully developed, instead, it uses an established flow velocity distribution at the entrance of the heated segment. Additionally, the solid walls are assumed to have no slip. The conditions and properties of the fluid used in the analysis are listed in Table 1.

Numerical investigation of subcooled nucleate flow boiling in a rectangular channel with dual heated walls, using FC-72 as the working fluid. The study encompassed three distinct mass velocities and a range of wall heat fluxes spanning from 42% to 45% of the Critical Heat Flux.

Table 1: Input conditions of the three test cases

Study	1	2	3
Mass Velocity G (kg/m ² s)	445.8	836.6	2432.5
Fluid inlet temperature T_{in} (K)	300.97	304.54	309.02
Wall heat flux q'' (W/m ²)	146,301	191,553	194,873

2.5 Phase Change Model

The ability to predict heat and mass transfer accurately relies on using the right phase change model. Commonly employed models such as that of Schrage [31], Tanasawa [32] and Lee [33] were initially considered. Schrage's model, although highly accurate, is not applicable for the current computations when the channel contains only liquid initially, as it relies on the presence of a boundary separating the two different phases. Tanasawa's improved version of Schrage's model incorporates slight variations in interface temperature compared to the saturation temperature and assumes a linear relationship between interfacial mass flux and interface superheat. However, it also necessitates the presence of an interface, which is not relevant to this particular study. On the other hand, the Lee model demonstrates effectiveness in predicting phase change within the bulk flow when the fluid temperature surpasses saturation. This

characteristic enables the Lee model to anticipate the spatial progression of flow boiling throughout the channel, commencing from a fluid state devoid of vapor. Hence, the Lee model was selected to calculate the phase change induced mass transfer in this study.

The mass transfer rate per unit volume is given by

$$\dot{m}_{fg} = r_i \alpha_f \rho_f \frac{(T_f - T_{sat})}{T_{sat}} \text{ for evaporation } (T_f > T_{sat}) \text{ and}$$

$$\dot{m}_{gf} = r_i \alpha_g \rho_g \frac{(T_{sat} - T_g)}{T_{sat}} \text{ for condensation } (T_g < T_{sat}),$$

The mass transfer intensity factor, denoted as r_i , is an empirical coefficient that varies for different evaporation and condensation setups. Assigning the correct value for r_i is a significant challenge when utilizing the Lee model because it greatly affects the predictions of wall temperature. Furthermore, r_i has a profound impact on various aspects of interfacial behavior within the flow channel, such as bubble diameters, interfacial area, and the exchange of molecules between phases.

Determining the right value of r_i for a specific scenario is typically not known beforehand. Selecting an overwhelmingly elevated r_i value can lead to numerical convergence problems, whereas a smaller r_i value will lead to significant deviations between interfacial and saturation temperatures.

Table 2: Corresponding thermophysical properties of FC-72 used in the three test cases

G (kg /m ² s)	T_{sat} (K)	h_{fg} (J /kgmol)	ρ_f (kg /m ³)	$c_{p,f}$ (J /kg · K)	k_f (W /m · K)	μ_f (kg /m · s)	ρ_g (kg /m ³)	$c_{p,g}$ (J /kg · K)	k_g (W /m · K)	μ_g (kg /m · s)
Case 1 445.75	333.3	2.760 $\times 10^7$	1605.2	1120.1	0.053	3.78 $\times 10^{-4}$	16.59	946.9	0.014	1.21 $\times 10^{-5}$
Case 2 836.64	335.3	2.974 $\times 10^7$	1608.2	1117.6	0.053	3.84 $\times 10^{-4}$	15.99	942.8	0.014	1.21 $\times 10^{-5}$
Case 3 2432.51	342.5	2.700 $\times 10^7$	1589.6	1133.1	0.052	3.49 $\times 10^{-4}$	19.95	967.9	0.014	1.24 $\times 10^{-5}$

Table 3: Numerical details and discretization methods.

Pressure-velocity coupling	Pressure-implicit with splitting of operators (PISO)
Gradient	Least squares cell based
Pressure	PRESTO!
Momentum	Third-order monotonic upstream-centered scheme for conservation laws (MUSCL)
Volume fraction	Geo-reconstruct
Turbulent kinetic energy	First-order upwind
Specific dissipation rate	First-order upwind
Energy	Second-order upwind
Transient formulation	First-order implicit

3. Results and Discussions

3.1 Flow Characteristics in sub-cooled boiling

We consider the experimental data from study of Lee et al. [30] and computational results of my simulation done in ANSYS FLUENT of test case 2 ($G = 836.6 \text{ kg/m}^2\text{s}$) only out of the three because of physical evidence obtained from literature where this intermediate mass-velocity test case has a mass intensity factor that results in good agreement between experimental and computational values.

3.1.1 Results of Flow Visualization

Here we present a comparison between experimental from Lee et. al [30] and computationally acquired visualization of flow boiling in a vertical up-flow channel with highly subcooled inlet

conditions. The visualization shows the temporal tracking of the interfacial behavior at mass velocities ($G = 836.6 \text{ kg/m}^2\text{s}$) with $\Delta t = 10 \text{ ms}$ intervals between each image. The findings indicate that the experimental observations of vapor bubble formation and the changes in interfacial phenomena throughout the thermally enhanced section of the channel are accurately predicted. The images demonstrate that the flow initially enters the channel inlet as single phase liquid, and vapor voids start forming throughout the thermally enhanced walls located slightly further along the flow path from the entrance region. As the bulk liquid gradually heats up, the vapor voids accumulate axially due to coalescence and decreasing condensation. Vapor voids further along the flow path combine with incoming vapor, eventually separating from the wall and entering the liquid core. The visual observations also indicate that although the vapor dynamics near the walls exhibit predominantly symmetrical patterns in the simulations, there are subtle variations between the two walls, possibly resulting from minor disturbances caused by turbulence.

The estimation of the experimental void fraction, obtained from existing literature, involves analyzing images using image processing techniques. It assumes that the bubble shape is either spherical, partially spherical with a flattened top, or partially spherical with an elliptical top. Figure 4 illustrates that the void fraction begins at a low value of 1–2% at the initial axial location and incrementally grows. It is worth noting the void fraction determined through measurements starts to rise with more rapidity around $z = 60 \text{ mm}$, coinciding with the presence of larger bubbles. Overall, the computed results align well with the experimental data, although they slightly overestimate the measurements due to the assumption of cylindrical rather than spherical vapor bubble shapes in the 2D domain. Furthermore, the experimentally derived relationships yield slightly variant predictions but still demonstrate satisfactory concurrence with both the empirical data and the computational models.

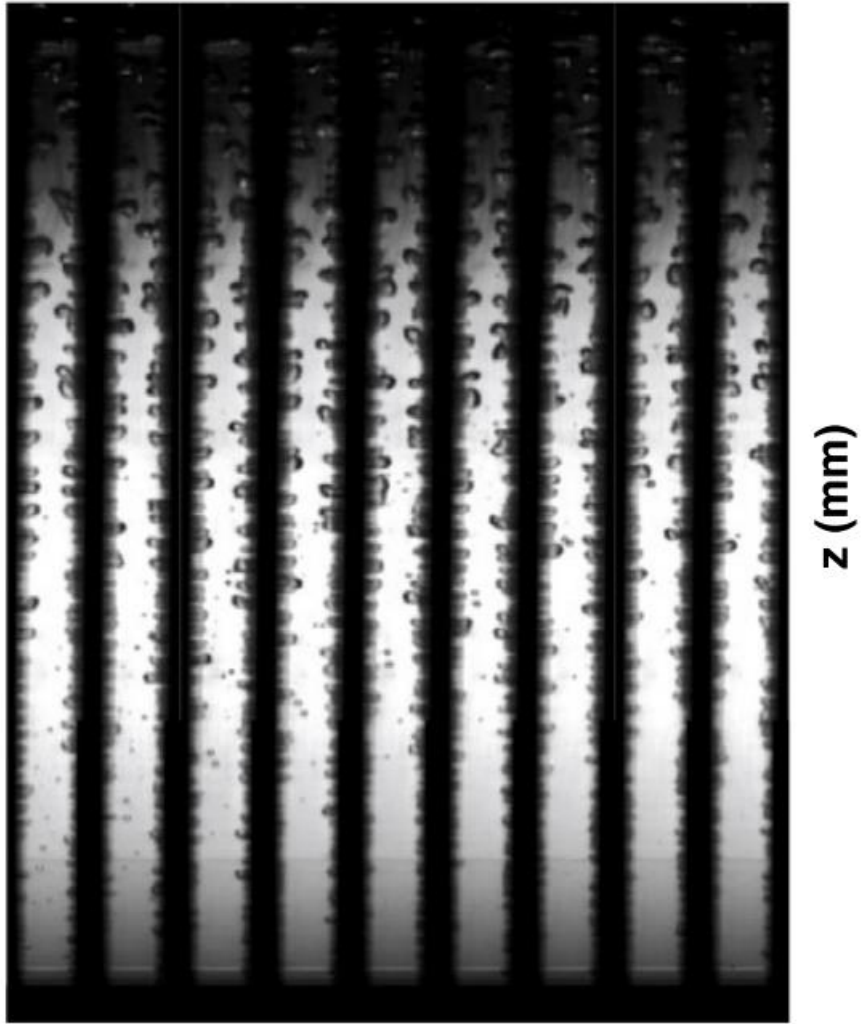


Figure 3: Experimental [30] flow images of channel at 10ms time apart in test case 2 [$G = 836.64 \text{ kg/m}^2\text{s}$]

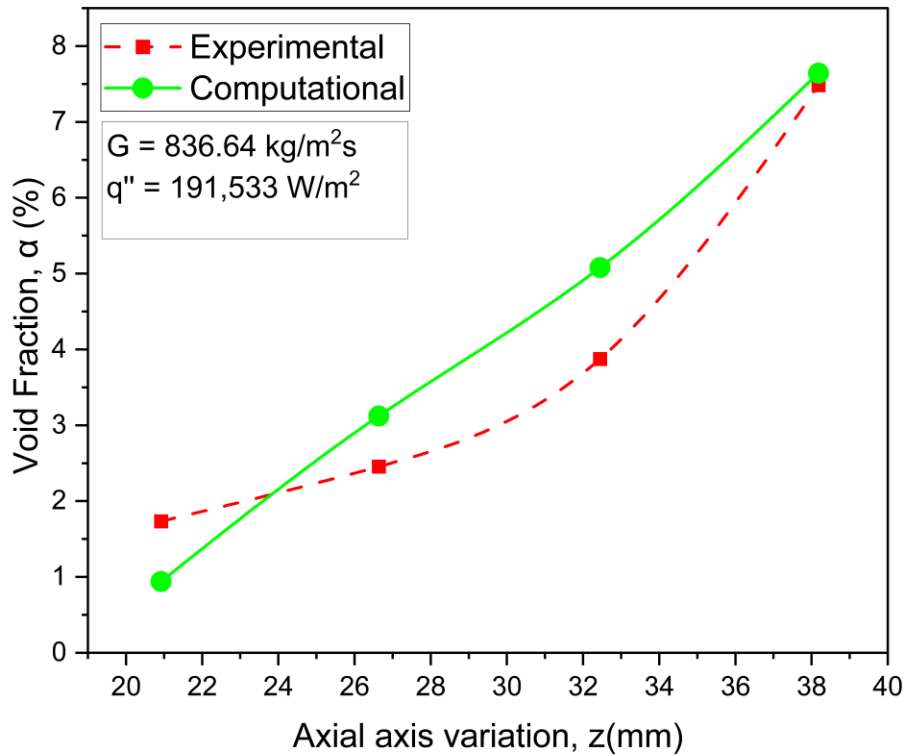


Figure 4: Analyzing for test Case 2 by Evaluating the Consistency between Empirical and Computational Axial Profiles of Average Void Fraction

3.1.2 Distribution of void fraction and velocity profiles in the transverse and longitudinal directions of the channel

Gaining insights into the interface dynamics within the channel necessitates examining the spatial variations of void fraction and flow velocity along the channel. Emphasizing the symmetrical characteristics of the velocity distribution at the inlet and the magnitude of the heat flux applied to both heated surfaces is of utmost importance. Consequently, any asymmetry detected in the simulation outcomes can be attributed to localized vapor void formation inside the channel. Figure 5 presents profile predictions for the transverse void profile across various axial positions within the channel for test case 2, depicting how the void fraction profiles resemble those typically seen in bubbly flow with a subcooled liquid core. Initially, at the upstream location, the void fraction is zero, indicating the absence of vapor generation. However, at the second axial location, there is a peak void fraction near the wall and decreased vapor volume fraction close to the central axis, suggesting the presence of a bubble layer in near proximity to the wall whereas the majority of the channel core is occupied

by liquid. At the third and fourth axial positions, when the mass velocities are at their lowest and intermediate levels, the vapor layer extends closer to the centerline due to the expansion and merging of vapor voids caused by the incremental warming of the middle liquid region.

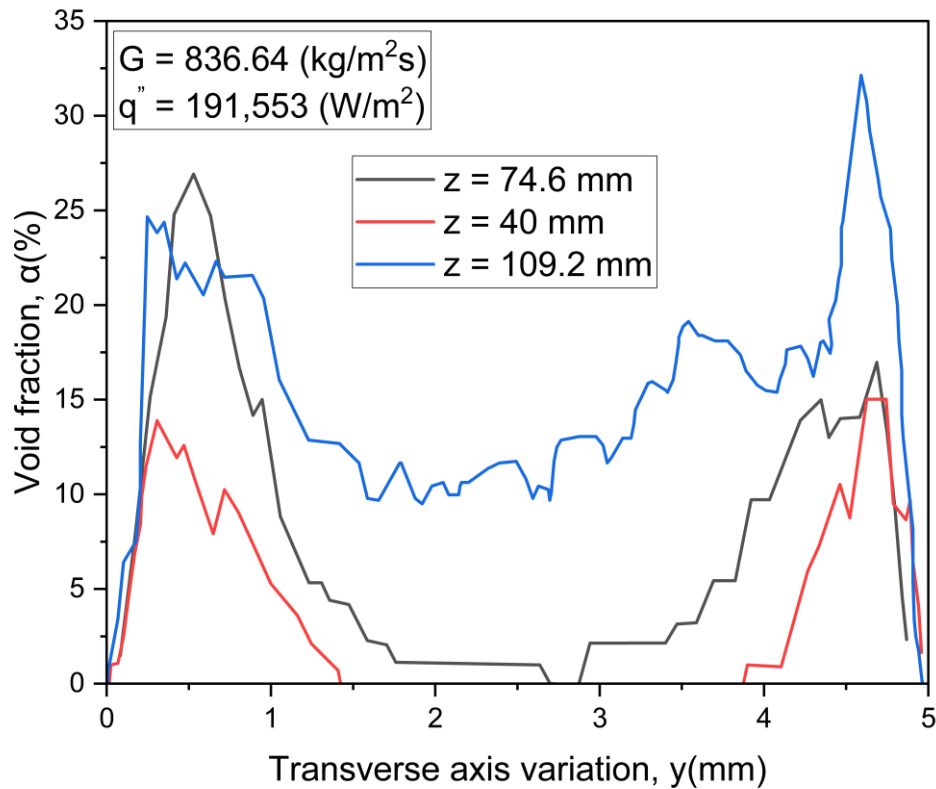


Figure 5: Comparison of time-averaged transverse void fraction profile along different axial locations

3.2 Heat transfer characteristics in sub-cooled boiling

By examining experimental images, it was observed that the entrance region dominated by liquid phase heat convection, heat flux occurred for the minimum mass velocity of $G = 445.75$ kg/m²s [test case 1]. The characteristics of the thermal boundary layer changed when bubble nucleation began, resulting in the dissipation of heat from the solid to the fluid through nucleate boiling. As the bubbles expanded and separated from the surface, areas of elevated temperature expanded towards the midline of the channel. In the region located further along the flow path, heat transfer primarily occurred through nucleate boiling. Turbulent effects caused by the motion of bubbles led to a disordered temperature field downstream, indicating an increase in

convective heat transfer. In the entrance region, the wall temperature increased due to the axial warming of the liquid, which is the point at which the heat flux in single-phase is more pronounced. However, within the nucleate boiling region, the wall temperature remained consistent, ranging between 346 and 351 K. Although there was an overprediction of approximately 7 K compared to the measurements, the computational model exhibited high precision across the entire length of the heated channel segment. For the test case 2, mass velocity of $G = 836.64 \text{ kg/m}^2\text{s}$, Figure 6 displayed similar axial variations in the predicted wall temperature as in test case 1, with reasonable accuracy in predicting the temperature data.

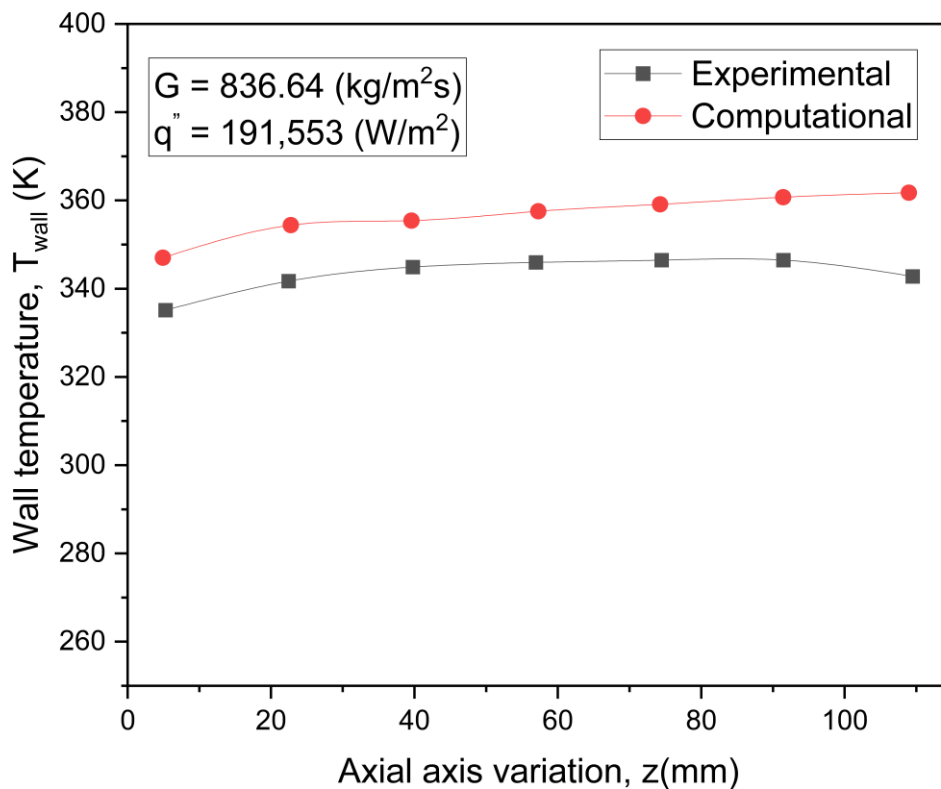


Figure 6: Comparison of experimental and computational axis variations of wall temperature for test case 2

Figure 7 illustrates the variations of the local heat transfer coefficient, h , along the axial direction for a gas mass velocity (G) of $836.64 \text{ kg/m}^2\text{s}$ and heat fluxes ranging from 42% to 45% of the Critical Heat Flux (CHF). The predicted values of h , similar to the wall temperatures, are time-averaged over a steady-state period of one second. Due to the challenges associated with experimental measurement, the fluid temperature at each axial location is determined through a straightforward energy balance within a control volume. Upon

comparing the calculated heat transfer coefficients to their experimental counterparts, it is evident that the calculated values generally exhibit a tendency to underestimate the experimental values. The extent of underestimation varies depending on the mass velocity. In the upstream region, the measured heat transfer coefficient (h) decreases due to the formation of a thermal boundary layer in a predominantly liquid phase dominated flow. However, in the middle region, it remains relatively constant, and in the exit region, it increases once again as a result of axial acceleration caused by an increased void fraction. This acceleration effect is more pronounced for test case 1, leading to more significant increases in h compared to test case 3.

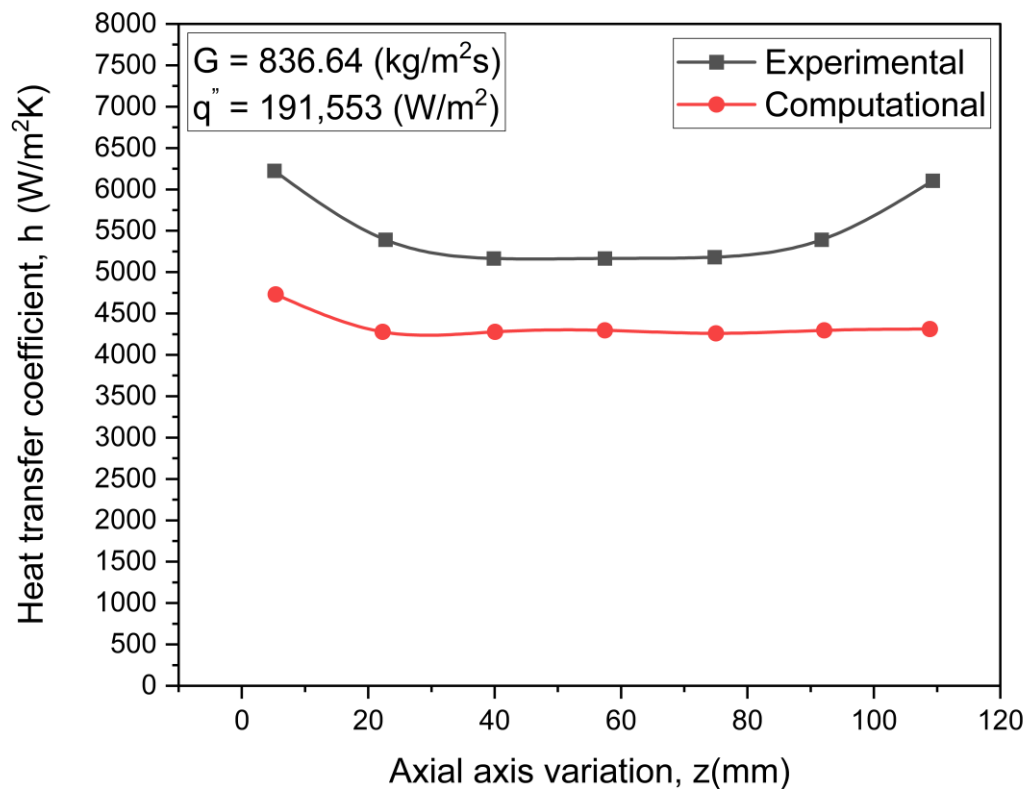


Figure 7: Comparison of experimental and computational axis variations of local heat transfer coefficient for test case 2

For $G = 836.64$ kg/m²s, the predicted h values shown in Figure 7 capture the decrease at the inlet and the relatively flat profile in the middle, but they persist as flat profiles toward the outlet and fail to capture the downstream enhancement. The predicted h values also slightly underestimate the measured values. To draw a conclusion, the computationally acquired model

demonstrates good efficacy in anticipating wall temperatures and heat transfer coefficients. However, as the mass velocities escalate, the disparities between projected and measured values tend to grow.

These disparities can be ascribed to the constraints associated with the two-dimensional (2D) domain employed in the simulations. In contrast to the tangible process of boiling, the two-dimensional approach proves ineffective to accurately depict the true morphology of bubbles, resulting in a smaller projected area in contact with the liquid phase. Furthermore, the simulations neglect the three-dimensional turbulence effects that affect fluid mixing and the motion of vapor bubbles. Another limitation lies in the absence of shear stress generated by the adiabatic side heating walls, which becomes increasingly significant as the mass velocity increases.

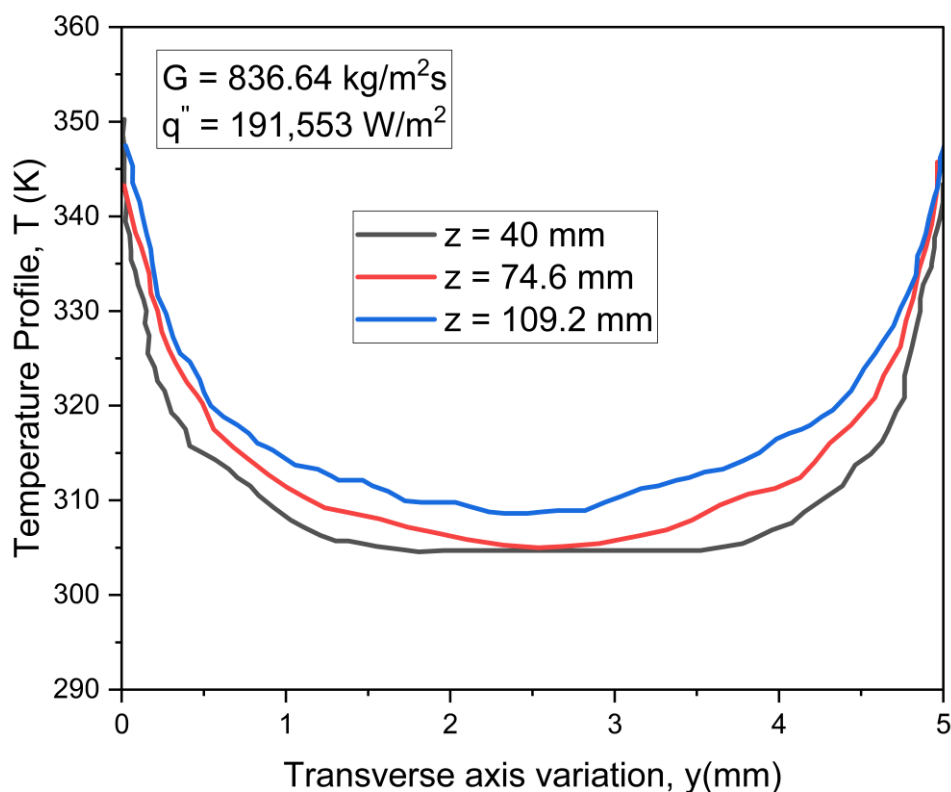


Figure 8: Differences in the temperature distribution within the channel at three specific axial positions for test case 2.

Figure 8 illustrates the variations in locally averaged temperature profiles within the channel

at three different axial locations corresponding to a mass velocity of $G = 836.64 \text{ kg/m}^2\text{s}$. The process of temporal averaging is performed for a duration of one second after achieving a steady state, similar to the approach used in Figure 7 to calculate the area-weighted temperature average.

In the sections closer to the inlet, the fluid domain primarily contains Coolant below saturation temperature at 301 K, exhibiting a substantial thermal variation in proximity to the channel walls. Progressing along the channel, the core temperature noticeably increases while the temperature gradient near the wall decreases. Beyond the distance of $z = 40.0 \text{ mm}$, the temperature near the wall exceeds the saturation temperature ($T_{\text{sat}} = 333.31 \text{ K}$), indicating that the region of elevated temperature extending further with increasing distance. The temperature profiles downstream exhibit some fluctuations, attributed to the presence of vapor voids with higher temperatures within the liquid region. In test case 2 mass velocity of $G = 836.64 \text{ kg/m}^2\text{s}$, Figure 8 depicts similar trends in the temperature mix across the channel, because the flow regime is quite similar to that of test case 1. The increase of temperature of channel core region is not significant while the temperature gradients of heating walls is much more significant compared to test case 1.

4. Future Work

Employing a higher mesh quality and lower step size for numerical computations to achieve a more accurate result. Using user-defined function for variable property functions of FC-72 in ANSYS fluent model's fluid property selection section. Gathering more data about similar experiments to compare the simulation model with real world images using advanced image processing tools. Calculate the heat transfer of different configurations by measuring the thermal conduction factor throughout the model's longitudinal span. Employing more computational power to further processing of test cases using more time steps.

5. Conclusions

The focus of this study was to examine the subcooled nucleate flow boiling of a certain fluid, FC-72, in a vertical up flow rectangular channel with heat fluxes applied to opposite walls. Both experimental and computational methods were used to gather data and predictions were made using a specific software and a phase change model. These predictions were then compared to experimental results and prior correlations to evaluate the accuracy of the methodology used. This research also examined challenging-to-measure phenomena, such as vapor fraction, flow velocity distribution, and localized mixture temperature. The results show that the methodology used is capable of representing the physical flow boiling processes observed, but the accuracy decreases for high mass velocities due to limitations of treating the nucleate flow boiling as a 2D process. Further research in this field could involve utilizing more computational resources to allow for a 3D domain.

References

- [1] “Flow Boiling and Condensation Experiment (FBCE),” *Glenn Research Centre, NASA*. <https://www1.grc.nasa.gov/space/iss-research/iss-fcf/fir/fbce/> (accessed Jun. 08, 2023).
- [2] V. S. Devahdhanush, Y. Lei, Z. Chen, and I. Mudawar, “Assessing advantages and disadvantages of macro- and micro-channel flow boiling for high-heat-flux thermal management using computational and theoretical/empirical methods,” *Int J Heat Mass Transf*, vol. 169, Apr. 2021, doi: 10.1016/j.ijheatmasstransfer.2020.120787.
- [3] J. Lee and I. Mudawar, “Fluid flow and heat transfer characteristics of low temperature two-phase micro-channel heat sinks - Part 1: Experimental methods and flow visualization results,” *Int J Heat Mass Transf*, vol. 51, no. 17–18, pp. 4315–4326, Aug. 2008, doi: 10.1016/j.ijheatmasstransfer.2008.02.012.
- [4] R. J. Weatherhead, “NUCLEATE BOILING CHARACTERISTICS AND THE CRITICAL HEAT FLUX OCCURRENCE IN SUBCOOLED AXIAL-FLOW WATER SYSTEMS,” Argonne, IL (United States), Mar. 1963. doi: 10.2172/4727562.
- [5] L. Consolini and J. R. Thome, “Micro-channel flow boiling heat transfer of R-134a, R-236fa, and R-245fa,” *Microfluid Nanofluidics*, vol. 6, no. 6, pp. 731–746, Jun. 2009, doi: 10.1007/s10404-008-0348-7.
- [6] W. R. Chang, C. A. Chen, J. H. Ke, and T. F. Lin, “Subcooled flow boiling heat transfer and associated bubble characteristics of FC-72 on a heated micro-pin-finned silicon chip,” *Int J Heat Mass Transf*, vol. 53, no. 23–24, pp. 5605–5621, Nov. 2010, doi: 10.1016/j.ijheatmasstransfer.2010.05.014.
- [7] X. Hu, G. Lin, Y. Cai, and D. Wen, “Experimental study of flow boiling of FC-72 in parallel minichannels under sub-atmospheric pressure,” in *Applied Thermal Engineering*, Dec. 2011, pp. 3839–3853. doi: 10.1016/j.applthermaleng.2011.07.032.
- [8] I. Mudawar, “Flow Boiling and Flow Condensation in Reduced Gravity,” in *Advances in Heat Transfer*, Academic Press, 2017, pp. 225–306. doi: 10.1016/bs.aiht.2017.06.002.
- [9] C. R. Kharangate and I. Mudawar, “Review of computational studies on boiling and condensation,” *International Journal of Heat and Mass Transfer*, vol. 108. Elsevier Ltd, pp. 1164–1196, 2017. doi: 10.1016/j.ijheatmasstransfer.2016.12.065.
- [10] H. Zhang, I. Mudawar, and M. M. Hasan, “Flow boiling CHF in microgravity,” *Int J Heat Mass Transf*, vol. 48, no. 15, pp. 3107–3118, Jul. 2005, doi:

- 10.1016/j.ijheatmasstransfer.2005.02.015.
- [11] V. Baturkin, “Micro-satellites thermal control—concepts and components,” *Acta Astronaut*, vol. 56, no. 1–2, pp. 161–170, Jan. 2005, doi: 10.1016/j.actaastro.2004.09.003.
- [12] M. K. Sung and I. Mudawar, “Single-Phase and Two-Phase Hybrid Cooling Schemes for High-Heat-Flux Thermal Management of Defense Electronics,” *J Electron Packag*, vol. 131, no. 2, Jun. 2009, doi: 10.1115/1.3111253.
- [13] Hui Zhang, I. Mudawar, and M. M. Hasan, “Application of Flow Boiling for Thermal Management of Electronics in Microgravity and Reduced-Gravity Space Systems,” *IEEE Transactions on Components and Packaging Technologies*, vol. 32, no. 2, pp. 466–477, Jun. 2009, doi: 10.1109/TCAPT.2008.2004413.
- [14] G. Research Assistant, “I. Mudawar Parametric Investigation Into the Effects of Pressure, Subcooling 3 Surface Augmentation and Choice of Coolant on Pool Boiling in the Design of Cooling Systems for High-Power-Density Electronic Chips,” 1990. [Online]. Available: <http://www.asme.org/about-asme/terms-of-use>
- [15] W. Yu, D. M. France, M. W. Wambsganss, and J. R. Hull, “Two-phase pressure drop, boiling heat transfer, and critical heat flux to water in a small-diameter horizontal tube.” [Online]. Available: www.elsevier.com/locate/ijmulflow
- [16] C. B. Tibirićá and G. Ribatski, “Flow boiling in micro-scale channels – Synthesized literature review,” *International Journal of Refrigeration*, vol. 36, no. 2, pp. 301–324, Mar. 2013, doi: 10.1016/j.ijrefrig.2012.11.019.
- [17] J. R. Thome and A. Cioncolini, “Flow Boiling in Microchannels,” in *Advances in Heat Transfer*, Academic Press, 2017, pp. 157–224. doi: 10.1016/bs.aiht.2017.06.001.
- [18] T. SATO and H. MATSUMURA, “On the Conditions of Incipient Subcooled-Boiling with Forced Convection,” *Bulletin of JSME*, vol. 7, no. 26, pp. 392–398, 1964, doi: 10.1299/jsme1958.7.392.
- [19] J. T. Rogers, M. Salcudean, Z. Abdullah, D. McLeod, and D. Poirier, “The onset of significant void in up-flow boiling of water at low pressure and velocities,” *Int J Heat Mass Transf*, vol. 30, no. 11, pp. 2247–2260, Nov. 1987, doi: 10.1016/0017-9310(87)90218-3.
- [20] S. E.-D. El-Morshedy, “Predictive study of the onset of flow instability in narrow vertical rectangular channels under low pressure subcooled boiling,” *Nuclear Engineering and Design*, vol. 244, pp. 34–42, Mar. 2012, doi:

- 10.1016/j.nucengdes.2011.12.019.
- [21] H. Zhang, I. Mudawar, and M. M. Hasan, “Flow boiling CHF in microgravity,” *Int J Heat Mass Transf*, vol. 48, no. 15, pp. 3107–3118, Jul. 2005, doi: 10.1016/j.ijheatmasstransfer.2005.02.015.
- [22] S.-M. Kim and I. Mudawar, “Review of databases and predictive methods for heat transfer in condensing and boiling mini/micro-channel flows,” *Int J Heat Mass Transf*, vol. 77, pp. 627–652, Oct. 2014, doi: 10.1016/j.ijheatmasstransfer.2014.05.036.
- [23] S.-M. Kim and I. Mudawar, “Universal approach to predicting two-phase frictional pressure drop for mini/micro-channel saturated flow boiling,” *Int J Heat Mass Transf*, vol. 58, no. 1–2, pp. 718–734, Mar. 2013, doi: 10.1016/j.ijheatmasstransfer.2012.11.045.
- [24] C. R. Kharangate and I. Mudawar, “Review of computational studies on boiling and condensation,” *International Journal of Heat and Mass Transfer*, vol. 108. Elsevier Ltd, pp. 1164–1196, 2017. doi: 10.1016/j.ijheatmasstransfer.2016.12.065.
- [25] F. Durst, D. Miloievic, and B. Schönung, “Eulerian and Lagrangian predictions of particulate two-phase flows: a numerical study,” *Appl Math Model*, vol. 8, no. 2, pp. 101–115, Apr. 1984, doi: 10.1016/0307-904X(84)90062-3.
- [26] C. W. Hirt and B. D. Nichols, “Volume of fluid (VOF) method for the dynamics of free boundaries,” *J Comput Phys*, vol. 39, no. 1, pp. 201–225, Jan. 1981, doi: 10.1016/0021-9991(81)90145-5.
- [27] “ANSYS Fluent User’s Guide,” 2020. [Online]. Available: <http://www.ansys.com>
- [28] J. U. Brackbill, D. B. Kothe, and C. Zemach, “A continuum method for modeling surface tension,” *J Comput Phys*, vol. 100, no. 2, pp. 335–354, Jun. 1992, doi: 10.1016/0021-9991(92)90240-Y.
- [29] J. Lee, S. Kim, and I. Mudawar, “Assessment of computational method for highly subcooled flow boiling in a horizontal channel with one-sided heating and improvement of bubble dispersion,” *International Journal of Thermal Sciences*, vol. 184, p. 107963, Feb. 2023, doi: 10.1016/j.ijthermalsci.2022.107963.
- [30] J. Lee, L. E. O’Neill, S. Lee, and I. Mudawar, “Experimental and computational investigation on two-phase flow and heat transfer of highly subcooled flow boiling in vertical upflow,” *Int J Heat Mass Transf*, vol. 136, pp. 1199–1216, Jun. 2019, doi: 10.1016/j.ijheatmasstransfer.2019.03.046.
- [31] R. W. Schrage, *A Theoretical Study of Interphase Mass Transfer*. Columbia University

- Press, 1953. doi: 10.7312/schr90162.
- [32] I. Tanasawa, “Advances in Condensation Heat Transfer,” 1991, pp. 55–139. doi: 10.1016/S0065-2717(08)70334-4.
- [33] “A Pressure Iteration Scheme for Two-Phase Flow Modeling,” in *Computational Methods for Two-Phase Flow and Particle Transport*, WORLD SCIENTIFIC, 2013, pp. 61–82. doi: 10.1142/9789814460286_0004.